

Shape of rotating quasiparticle orbits and signature splitting in La, Ce, and Pr nuclei

Y. S. Chen* and S. Frauendorf†

Department of Physics, University of Tennessee, Knoxville, Tennessee 37916

G. A. Leander

UNISOR, Oak Ridge Associated Universities, Oak Ridge, Tennessee 37830

(Received 23 June 1983)

A simple semiclassical picture of the rotating spatial density distribution for spin-aligned high- j quasiparticles emerges from the cranking model. Evidence for the physical relevance of this picture can be sought in the signature splitting of rotational bands in γ -soft nuclei. The cerium region is a suitable testing ground, and model calculations are presented for bands which might be observed experimentally.

NUCLEAR STRUCTURE Cranking model. Triaxiality of rotating quasiparticle orbitals. Calculated effect on signature splitting in high spin bands of $^{129-133}\text{La}$, $^{129-135}\text{Ce}$, $^{131-135}\text{Pr}$.

I. INTRODUCTION

Nuclear structure at high spin is often described on the basis of a semiclassically rotating average field, i.e., an intrinsic shape turning uniformly around a fixed axis in space.¹ The physical consequences of such motion depend critically on the shape asymmetry in the plane of rotation, which determines the time dependence of the nuclear and Coulomb fields.² The intrinsic shape is characterized to lowest order by the quadrupole asphericity, ϵ , and triaxiality, γ —the asymmetry in the plane of rotation depends on both of these shape coordinates.^{3,4} Therefore it is desirable to measure, among other things, a quantity which is sensitive specifically to one of them. Such a probe is provided by nucleons in high- j rotation-aligned orbitals because, in rotational bands with spin contributions from such orbitals, the two sets of alternating spin states are displaced in energy by an amount which depends sensitively on the triaxiality γ .^{5,6} Recent studies of the cranked shell model have opened broader perspectives for the possible use of this mechanism.⁷⁻¹² In particular it was suggested that changes in the energy staggering between alternate spin states could be used to trace out the evolution of γ at high spins. Furthermore, it should be possible to identify a departure from the collective rotational sector, $0^\circ > \gamma > -60^\circ$ by the Lund convention,³ toward the single-particle rotational limit at $\gamma = -120^\circ$ or $+60^\circ$.

Attempts to interpret experimental data by this mechanism could help determine the limits on the validity of the cranked mean field approximation. This is especially the case for systems not too far from the closed shells, which are soft with respect to the γ shape degree of freedom if the concept of shape is appropriate at all. The present paper reports a theoretical estimate of effects which would arise from triaxiality in the cerium region and which could be looked for by γ -ray spectroscopy with heavy ions. First the physical origin of these effects will be visualized.

II. INITIAL CONSIDERATIONS

A. Triaxiality of rotating quasiparticle orbits

The present emphasis is on effects from polarization in the γ degree of freedom due to the specific shape of high- j rotation-aligned orbitals. The systematics of how shape depends on the filling of a high- j shell is shown schematically in Fig. 1. It is well known that a single particle in a high- j shell generates a torus-shaped density distribution and thus tends to make the nucleus oblate with the spin along the symmetry axis, corresponding to $\gamma = +60^\circ$. A single hole goes into a similar orbit and tends to make the nucleus prolate with the spin along the symmetry axis, corresponding to $\gamma = -120^\circ$. The intermediate situation of a rotation-aligned quasiparticle in a half-filled j shell can be viewed as a hole on one part of its orbit and a par-

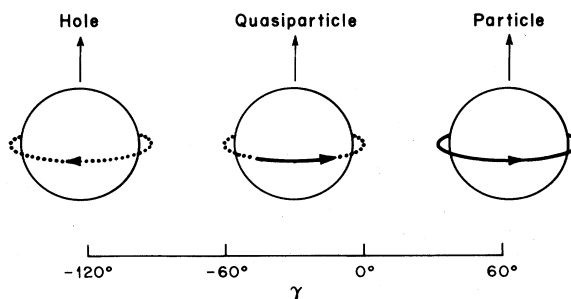


FIG. 1. Geometrical picture of rotation-aligned high- j quasiparticle orbits. A “particle” in an empty j shell or a “hole” in a filled j shell has a toroidal density distribution which tends to make the nucleus oblate ($+60^\circ$) or prolate (-120°), respectively, and symmetric around the rotation axis. A “quasiparticle” in a partly filled shell is particlelike on spatially localized sections of its orbit and holelike on the other sections, thereby helping to create a density bulge which can move slowly around the rotation axis as a collective rotation.

title on the other part, prone to generate an asymmetric density distribution. This we deduce from previous numerical results^{10,11} which show that as the filling of the shell varies from empty to full, a maximum overlap is achieved with a nuclear shape whose γ varies smoothly from $+60^\circ$ to -120° through all the intermediate triaxial shapes.

B. Signature splitting

Signature is the quantum number associated with symmetry under a rotation of π about the axis of nuclear rotation. The symmetry operator is $e^{-i\pi J_x}$ and the eigenvalues are $e^{-i\pi\alpha}$, where α is 0 or 1 for a system with integer spin and $-\frac{1}{2}$ or $\frac{1}{2}$ for a system with half-integer spin. Clearly α is additive modulo 2 for independent quasiparticles. The signature is directly observable because the allowed spins are $I = \alpha + 2n$ with n integer. Any splitting between the two signatures which is calculated in the cranking model should also be observable as an energy staggering between alternate spin states in a rotational band.

A direct connection between the geometrical picture of Fig. 1 and signature splitting comes about because Fig. 1 holds only for one of the two signatures, the "favored" signature of the j shell, $\alpha = j$ modulo 2. The orbits of the other signature correspond semiclassically to a quite different topology in phase space.¹³ Whereas the favored signature comes down in energy at the appropriate value of γ , the unfavored signature does not exhibit as marked preference for any particular γ value of the nucleus. Consequently, the signature splitting is large at the preferred γ of the favored signature, while at other γ values it is small and sometimes inverted. A systematic numerical demonstration of this effect was given in Ref. 11.

An example of a change in signature splitting which might be caused by γ shape polarization has been observed in the nuclei ^{81}Kr ,¹⁴ $^{155,157}\text{Ho}$,¹⁵ ^{159}Tm .¹⁶ In both cases a decrease in the signature splitting for a midshell quasiparticle ($\nu g_{9/2}$ in krypton, $\pi h_{11/2}$ in holmium and thulium) is observed when rotation-aligned orbits at the bottom of another shell ($\pi g_{9/2}$ in krypton, $\nu i_{13/2}$ in holmium and thulium) are occupied by two particles. The explanation according to the γ -polarization theory is that the latter particles tend to polarize the system toward $\gamma \geq 0^\circ$, away from the $\gamma \leq 0^\circ$ asymmetric shape which is preferred by the midshell quasiparticle in its favored signature states. However, the validity of this explanation and the generality of the mechanism are not yet established. For example, other dynamical effects might arise when rotational invariance is taken into account, or the residual interaction between the quasiparticles might alter the signature splitting. The latter has been suggested to be the case in some doubly odd nuclei.¹⁷ The relevance of the γ polarization mechanism should be tested by identifying some new clearcut situations. For example, a γ -inverse effect would be expected to occur when the rotation alignment is due to a pair of midshell quasiparticles, while the odd single particle occupies an empty j shell. Physically, the same thing would be observed as in the nuclei mentioned above, namely a decrease of the signature splitting after alignment. The mechanism, however, would be a

change of γ in the opposite direction, toward more negative γ values.

C. Testing grounds

Experimental tests of the kind described above are possible only in a few nuclides due to practical constraints. The core of the nucleus must be γ soft so that polarization can occur. The neutron-proton ratio must be suitable for the population of high spin states by heavy-ion reactions. In the example mentioned there must be a half-filled shell which gives rise to rotation alignment.

Some possible conjunctions of proton and neutron high- j shells are the following:

$\pi g_{9/2}, \nu g_{9/2}$. The case of ^{81}Kr was mentioned above.

$\pi g_{9/2}, \nu h_{11/2}$. A similar decrease of signature splitting appears in recently reported data on ^{103}Ag .¹⁸

$\pi h_{11/2}, \nu h_{11/2}$. The light Ce region is considered below.

$\pi h_{11/2}, \nu i_{13/2}$. The light Ho, Tm region is the most studied so far.⁷⁻¹⁰

$\pi h_{9/2}, \nu i_{13/2}$. Prolate and oblate shapes are believed to coexist in the light Hg cores, giving rise to different kinds of aligned structures at high spin in accord with the principles outlined above.¹⁹ The role of the mechanism discussed in the present paper was first noticed in a particle-rotor calculation²⁰ which showed that the $(i_{13/2})^1$ state in ^{185}Hg is oblate ($\gamma = -60^\circ$) specifically due to the Coriolis interaction. Still heavier collective nuclei are difficult to populate at high spins, and the very light nuclei do not provide long enough rotational bands. The Ce region is clearly favorable for studying a variety of γ -soft nuclei.

III. MODEL CALCULATIONS

A. The model

In order to obtain realistic estimates of the change in signature splitting to be expected from γ shape changes we consider a model¹⁰ where rotation-aligned quasiparticles from the cranking model are coupled to an empirical core, and a γ value is determined for each state by the variational method.

The quasiparticle states are obtained from the cranked Nilsson Hamiltonian with Bardeen-Cooper-Schrieffer (BCS) pairing²¹

$$h^\omega = h_{\epsilon, \epsilon_4}^{\text{Nilsson}}(\gamma) + \frac{1}{2} \Delta (P^+ + P) - \omega J_x, \quad (1)$$

where the shape coordinates ϵ, ϵ_4 and the pairing gap parameter Δ are held fixed at empirically reasonable values. A technical difficulty arises when quasiparticle levels cross in energy as a function of the triaxiality coordinate γ . If the crossing levels have the same quantum numbers, parity π , and signature α , there is in general an interaction between them. Then an adiabatic variation of γ changes one orbital into the other, and thereby spurious stationary points may arise in the energy as a function of γ at the crossings. We eliminate the spurious minima by hand, by drawing graphs of the quasiparticle levels as a function of γ (or ω , cf. Ref. 22) and replacing the calculated curves by smooth crossing lines through the interaction zones. A specified quasiparticle configuration can then be followed

to all values of ω and γ . The contribution, e^ω , from each quasiparticle to the energy in the rotating frame is obtained from the graphs.

The total energy in the rotating frame, the Routhian, includes in addition to the quasiparticles a number of phenomenologically parametrized contributions from the core

$$E^\omega = \sum e^\omega(\gamma) + \frac{1}{2} V_{po} \cos 3\gamma - \frac{1}{2} \omega^2 \mathcal{I} + e_\gamma n_\gamma. \quad (2)$$

The rationale for using a phenomenological core instead of one derived microscopically is familiar in the context of core-particle coupling. The analysis of observable effects due to the rotating quasiparticles can then be carried out with a core whose properties are optimally compatible with experimental facts. Also, empirical parameters ex-

tracted from the analysis are an interesting part of the results, useful for testing microscopic theories.

The second term on the right in Eq. (2) is the simplest possible potential energy function, with one parameter V_{po} equal to the prolate-oblate potential energy difference. The third term is the core rotational energy. The rotational moment of inertia, \mathcal{I} , is expressed by the two-parameter Harris formula times a hydrodynamical γ dependence

$$\mathcal{I} = (\mathcal{I}_0 + \frac{1}{2} \omega^2 \mathcal{I}_1)^{\frac{4}{3}} \cos^2(\gamma + 30^\circ). \quad (3)$$

The fourth term is used only for gamma bands ($n_\gamma = 1$). It stabilizes nonaxial shapes using the triaxial rotor formula for the energy of a gamma versus rotational 2^+ excitation

$$e_\gamma = E(2_{rot}^+) [(9 + \sqrt{81 - 72 \sin^2 3\gamma}) / (9 - \sqrt{81 - 72 \sin^2 3\gamma})]^{1/2}. \quad (4)$$

For any particular configuration and rotational frequency, ω , the Routhian, E^ω , is minimized numerically with respect to γ . If there are several local minima the higher ones are considered spurious, unless they correspond to different quasiparticle configurations. (A nominal quasiparticle configuration may include several true minima as a function of γ because only spurious minima and not maxima are eliminated.) From the results it is in principle possible to construct an excitation spectrum, but for the present purpose of finding the relative position of bands near yrast it is sufficient to obtain the Routhian.

B. The parameters

The calculation of quasiparticle levels requires six parameters: κ and μ , the spin-orbit and orbit-orbit strengths of the Nilsson model²³; ϵ and ϵ_4 , the absolute value of the quadrupole and hexadecapole shape coordinates; and λ and Δ , the Fermi level and the pairing gap parameter. The κ and μ values are taken from a general empirical formula²³ with a smooth dependence on mass number A .

The radial coordinate in the polar representation of quadrupole deformations is taken as $\epsilon = 0.25$ in the nuclei around ^{130}Ce , and $\epsilon = 0.21$ around ^{134}Ce , on the basis of measured $B(E2)$ and $E(2^+)$ systematics (see, e.g., the triaxial-rotor analysis of Gizon *et al.*²⁴). Cranking calculations have shown that the equilibrium value of ϵ changes very little in these nuclei up to the highest rotational frequencies of interest for discrete-line spectroscopy.²⁵

The hexadecapole radial coordinate ϵ_4 is taken from theoretical calculations^{26,27} of the ground-state equilibrium shape: $\epsilon_4 = 0.03$ and 0.02 around ^{130}Ce and ^{134}Ce , respectively. The γ dependence of the hexadecapole term in the Hamiltonian is fixed as in Ref. 28.

The Fermi level λ is determined by a BCS calculation for prolate shape and $\omega = 0$. Only the particle numbers corresponding to ^{130}Ce and ^{134}Ce are considered, and neighboring odd and doubly odd nuclei are obtained as quasiparticle excitations.

The BCS gap parameter Δ cannot be extracted empirically in the neutron-deficient cerium ($Z = 58$) region since

the experimental masses are not known. To check the reliability of theoretical values obtained with standard values of the pairing interaction strength we have compared theoretical odd-even mass differences from the Möller-Nix mass table²⁷ with experimental values in nuclei with lower Z where data are available. The agreement is good throughout the $50 < Z, N < 82$ region, with a notable exception for the most neutron-deficient isotopes of ^{55}Cs and ^{56}Ba , i.e., the nuclei deepest into the interior of this region and closest to ^{58}Ce which have known experimental masses. In Fig. 2 the experimental and theoretical

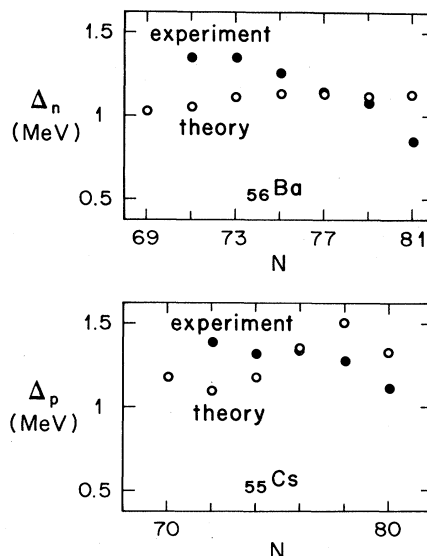


FIG. 2. The odd-even mass difference for neutrons in ^{56}Ba and protons in ^{55}Cs , taken from experiment and from the folded Yukawa model mass formula (Ref. 27). Note the anomalous increase of the experimental values toward the interior of the $50 < N < 82$ region. There is also an increase with Z , relative to ^{54}Xe and ^{53}I , respectively. Experimental data are not available for ^{57}La and ^{58}Ce .

odd-even mass differences for Cs and Ba are plotted versus neutron number N , and the discrepancy is seen to arise from an anomalously persistent increasing trend in the experimental values as N decreases from the magic number 82. The theoretical trend, which does not contain this effect, is the same for all nearby proton numbers both above and below $Z=55-56$. Thus the theoretical values for Ce are not very credible. It may be speculated, for example, that neutron-proton pairing becomes important in the interior of the $50 < Z, N < 82$ region. For the present calculations in the Ce region we simply set $\Delta_p = \Delta_n = 1.25$ MeV, following the experimental trend. This Δ_p value is also known²⁹ to be consistent with the backbending frequency in ^{130}Ce .

The core has four parameters: \mathcal{I}_0 and \mathcal{I}_1 of the variable moment of inertia formula; $E(2_{\text{rot}}^+)$, which scales the energy of the mode responsible for the γ band; and V_{po} , the prolate-oblate potential-energy difference.

Empirical values of \mathcal{I}_0 and \mathcal{I}_1 are given by the formula

$$\mathcal{I}^{(2)}(I) = \frac{I_x(I+1) - I_x(I-1)}{\omega(I+1) - \omega(I-1)} = \mathcal{I}_0 + 3\omega^2 \mathcal{I}_1 \quad (5)$$

in bands where four or more unperturbed levels are known.³⁰ These values may vary from one band to the other; however, a consistent set of Routhians must be based on one average set of values. We have checked that our main conclusions are not sensitive to the adopted values, which are determined empirically from the high-spin states without correction for γ effects. For nuclei around ^{134}Ce we use $\mathcal{I}_0 = 11.4\hbar^2 \text{ MeV}^{-1}$, $\mathcal{I}_1 = 29\hbar^4 \text{ MeV}^{-3}$, and for nuclei around ^{130}Ce we take $\mathcal{I}_0 = 21\hbar^2 \text{ MeV}^{-1}$, $\mathcal{I}_1 = 18\hbar^4 \text{ MeV}^{-3}$. It may be remarked that the \mathcal{I}_1 values for many known bands in $^{128-136}\text{Ce}$ and neighboring nuclides are larger, $\mathcal{I}_1 \sim 50\hbar^4 \text{ MeV}^{-3}$, but such

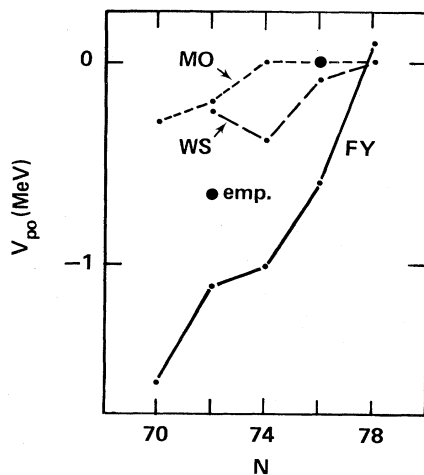


FIG. 3. The prolate-oblate potential-energy difference $V_{\text{po}} = V_p - V_0$ from deformed shell model theory and the present empirical analysis. The modified-oscillator (MO) and Woods-Saxon (WS) values were extracted with some uncertainty from diagrams in Refs. 26 and 31; the folded-Yukawa (FY) values based on Ref. 27 were communicated by Möller.

large values are not feasible at higher spins. For $E(2_{\text{rot}}^+)$ we use the measured energy of the 2^+ state in the ground band of the doubly even nucleus.

Theoretical calculations of V_{po} have an uncertainty of the order of 1 MeV, as is well known, e.g., from experience in the light mercury region. Results of some different calculations are shown in Fig. 3. Within the present model, an empirical handle on V_{po} is provided by the signature splitting in the $(\nu h_{11/2})^{-1}$ bands. The 109 keV splitting of the signatures observed for ^{131}Ce at $\omega = 250$ keV was reproduced using $V_{\text{po}} = -837$ keV. This value of V_{po} was adopted for the nuclei around ^{130}Ce . It lies between the theoretical curves in Fig. 3. For ^{134}Ce we used $V_{\text{po}} = 0$ in order to bring the experimentally observed³² neutron-aligned band down in energy. Additional evidence for γ instability comes from the $h_{11/2}$ spectrum of ^{133}La , which was very accurately predicted by coupling an $h_{11/2}$ particle to a γ -unstable core.³³

IV. RESULTS AND DISCUSSION

The Routhians which come lowest in energy after minimization with respect to γ are shown in Figs. 4–8. The bands are characterized as ground band (g.b.) or gamma band (γ) and by the number of neutron (ν) and proton (π) quasiparticles. In some cases the parity and signature are also indicated. More complete information is given in Table I. Results have been obtained only at selected rotational frequencies, $\omega = 0.03, 0.05, \text{ and } 0.07\hbar\omega_0$.

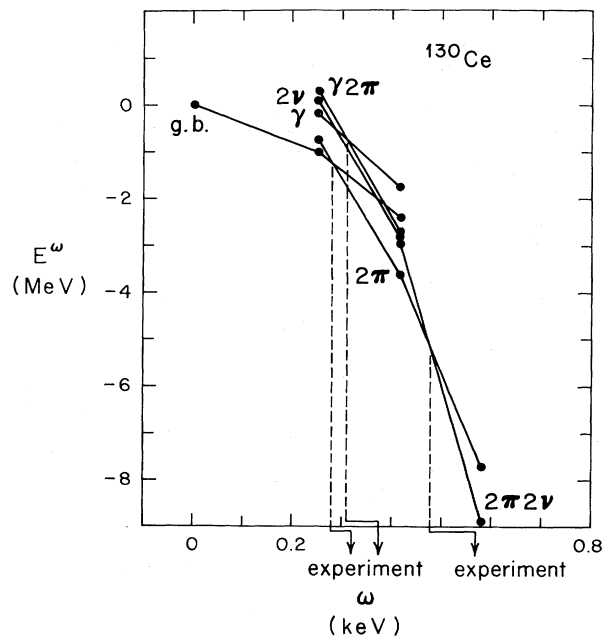


FIG. 4. Calculated Routhians for yrast and near-yrast bands in ^{130}Ce vs rotational frequency ω . Calculated points are connected by straight lines. Crossing points are related to experimental band crossing frequencies (Refs. 19 and 34). The number of neutron (ν) and proton (π) quasiparticles is indicated for each band. g.b. stands for ground band and γ for gamma band.

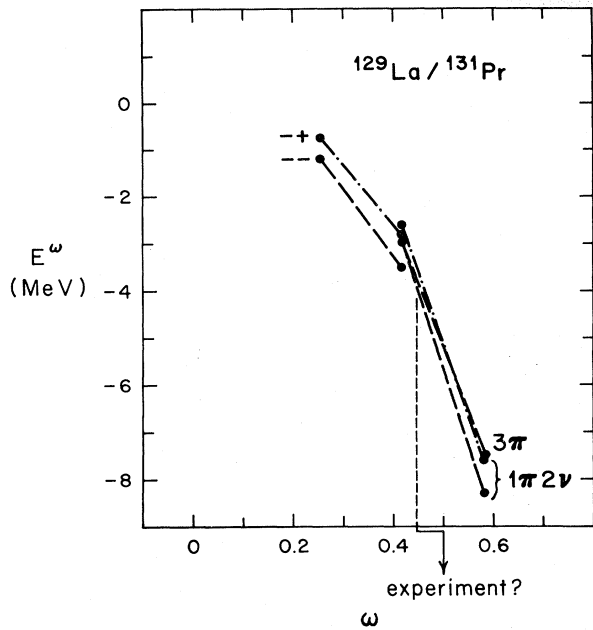


FIG. 5. Same as Fig. 4, but odd quasiproton bands. The parity and signature are also shown.

The objective of the following discussion is to note manifestations of γ shape polarization. The major effects are due to (i) the lowest proton $h_{11/2}$ quasiparticle of signature $\alpha = -\frac{1}{2}$, which is energy favored and has largest rotational alignment for $\gamma = 0^\circ$, collective rotation of a prolate shape; (ii) the corresponding neutron orbital which

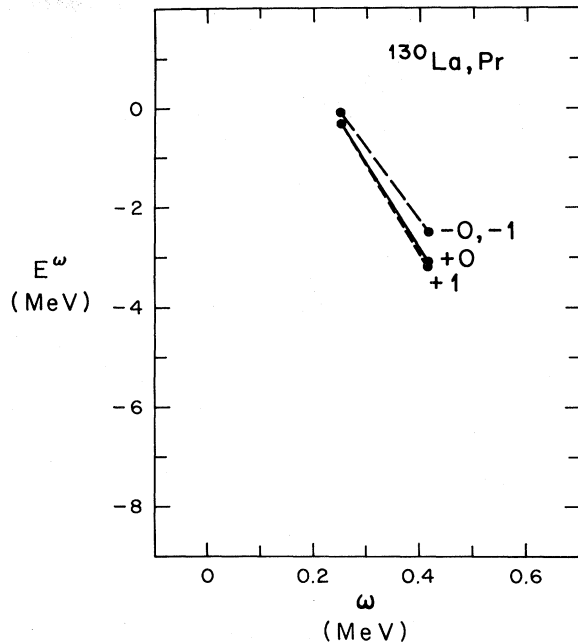


FIG. 7. Same as Fig. 4, but for bands with odd quasineutron and quasiproton numbers.

favors negative γ deformation; (iii) the core moment of inertia, which is taken to be largest at $\gamma = -30^\circ$; and (iv) the gamma mode which favors maximum triaxiality, $\gamma = +30^\circ, -30^\circ, \text{ or } -90^\circ$.

A. The nuclei around ^{130}Ce

(i) *The doubly even case, ^{130}Ce .* Experimental information which has recently become available³⁴ was taken into account in selecting the parameters of the present calculation. The first band crossing in Fig. 4 is due to proton

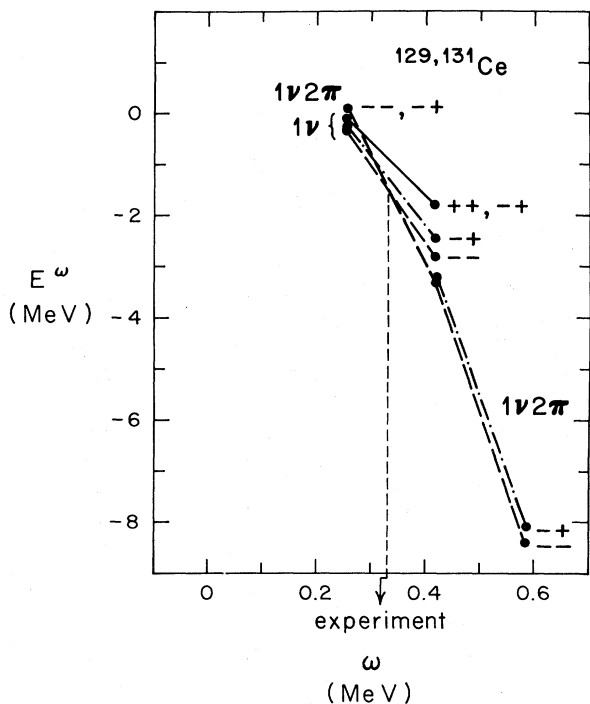


FIG. 6. Same as Fig. 4, but for odd quasineutron bands.

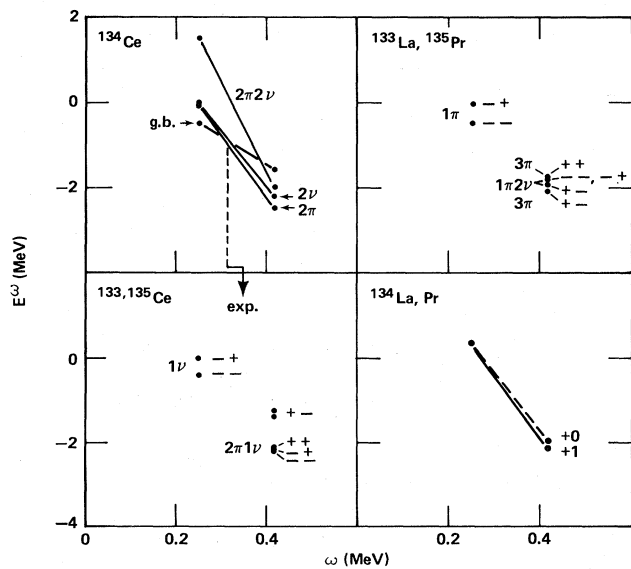


FIG. 8. Same as Figs. 4-7, but for ^{134}Ce .

TABLE I. Calculated γ deformation and signature splitting of the bands shown in Figs. 4–8. The description of the bands indicates the parity of individual neutron and proton quasiparticles, and separately the total parity and signature. The first entry for γ and the signature splitting is for the lowest frequency value ω , and subsequent entries in parentheses are for higher ω values. The sign of the signature splitting is defined here by taking the lower signature ($\alpha_{<}$) first.

	Band	Total parity	α	γ	$E_{\alpha_{<}}^{\omega} - E_{\alpha_{>}}^{\omega}$
^{130}Ce	g.b.	+	0	0(–7, –16)	
	γ	+	0	–28(–28)	
	$\gamma 2\pi^{-}$	+	0	–25(–25)	
	$2\nu^{-}$	+	0	–52(–43)	
	$2\pi^{-}$	+	0	–4(–8, –15)	
	$2\pi^{-} 2\nu^{-}$	+	0	–8(–20, –22)	
$^{130}\text{La, Pr}$	$1\pi^{-} 1\nu^{-}$	+	0	–7(–16)	–0.003(–0.114)
		+	1	–8(–20)	
	$1\pi^{-} 1\nu^{+}$	–	0	–6(–11)	–0.009(0.006)
		–	1	–6(–13)	
$^{129}\text{La, }^{131}\text{Pr}$	$1\pi^{-}$	–	$-\frac{1}{2}$	–6(–11)	–0.472(–0.696)
		–	$+\frac{1}{2}$	–7(–13)	
	$1\pi^{-} 2\nu^{-}$	–	$-\frac{1}{2}$	–40(–30)	–0.327(–0.693)
		–	$+\frac{1}{2}$	–25(–25)	
$^{129,131}\text{Ce}$	$1\nu^{-}$	–	$-\frac{1}{2}$	–45(–37)	–0.109(–0.398)
		–	$+\frac{1}{2}$	–15(–23)	
	$1\nu^{+}$	+	$-\frac{1}{2}$	–120(–22)	–0.012(–0.071)
		+	$+\frac{1}{2}$	–8(–14)	

alignment, as indicated by the data. In previous theoretical calculations^{11,25} the neutrons aligned before the protons because all quantities were derived within the Nilsson model which gives a smaller V_{po} and Δ_n smaller than Δ_p . A band crossing is also observed experimentally in the gamma band at larger frequency ω than in the yrast sequence, and with a larger interband interaction. The calculation produces a similar effect due to γ shape polarization. At the triaxial shape induced by the gamma mode (Table I) the proton spin alignment is reduced and the interaction matrix element is larger.

(ii) *The odd-proton case, ^{129}La or ^{131}Pr .* The alignment of neutrons at high spins gives rise to negative γ deformation and a subsequent reduction of the odd-proton signature splitting above the band crossing (Fig. 5). A similar reduction in signature splitting above the first band crossing has been observed, e.g., in ^{81}Kr (Ref. 14) and ^{159}Tm ,¹⁶ but there it is a change of γ in the opposite direction which could be responsible. It would be valuable to verify the “ γ inverse” of the ^{81}Kr , ^{159}Tm effect in an odd La or Pr isotope. Experimental difficulties might arise because the unfavored signature may not come down far enough in energy to be significantly populated. Other bands, for

example the $(\pi h_{11/2})^3$ band, are calculated to come very close to yrast in the region of the band crossing.

(iii) *The odd-neutron case, $^{129,131}\text{Ce}$.* The alignment of protons gives rise to an increase of γ and a subsequent reduction of the $h_{11/2}$ odd-neutron signature splitting according to the model (Fig. 6). This is the analog of the ^{81}Kr , ^{159}Tm effect, which can thus be looked for in the odd Ce isotopes. The one-quasiparticle $(\nu h_{11/2})^1$ signature splitting below the backbend involves very different γ deformations for the favored and unfavored signatures. The proton alignment occurs at a somewhat higher frequency than in ^{130}Ce , as for the ^{130}Ce gamma band mentioned above, and for the same reason, namely negative γ deformation. In the $^{129,131}\text{Ce}$ gamma bands the $h_{11/2}$ odd-neutron signature splitting is expected to be large due to the negative γ deformation.

(iv) *The doubly odd case, ^{130}La or Pr .* The conflicting γ -polarization effects from $h_{11/2}$ neutron and proton rotating quasiparticles give a reduction of the signature splitting relative to both the neutron and the proton one-quasiparticle case, as can be seen in Fig. 7, where the signature splitting is small. This should be feasible to check experimentally. The positive-parity band begins to split at

TABLE I. (Continued.)

	Band	Total parity	α	γ	$E_{\alpha_{<}}^{\omega} - E_{\alpha_{>}}^{\omega}$
^{134}Ce	$1\nu^{-}2\pi^{-}$	-	$-\frac{1}{2}$	$-6(-14, -21)$	-0.001(-0.100, -0.295)
		-	$+\frac{1}{2}$	$-6(-11, -17)$	
	$3\pi^{-}$	-	$-\frac{1}{2}$	$-6(-13)$	
	g.b.	+	0	$-30(-30)$	
	$2\pi^{-}$	+	0	$1(-10)$	
$^{134}\text{La, Pr}$	$2\nu^{-}$	+	0	$-69(-63)$	
	$2\pi^{-}2\nu^{-}$	+	0	$-64(-30)$	
	$1\pi^{-}1\nu^{+}$	+	0	$-11(-23)$	0.000(0.171)
		+	1	$-11(-29)$	
$^{133}\text{La}, ^{135}\text{Pr}$	$1\pi^{-}$	-	$-\frac{1}{2}$	-8	-0.410
		-	$+\frac{1}{2}$	-2	
	$1\pi^{-}2\nu^{-}$	-	$-\frac{1}{2}$	$-67(-55)$	0.001(-0.017)
		-	$+\frac{1}{2}$	$-67(-60)$	
	$1\pi^{+}2\nu^{-}$	+	$-\frac{1}{2}$	-59	-0.280
		+	$+\frac{1}{2}$	-67	
	3π	+	$-\frac{1}{2}$	-16	-0.303
		+	$+\frac{1}{2}$	-8	
$^{133,135}\text{Ce}$	$1\nu^{-}$	-	$-\frac{1}{2}$	-64	-0.434
		-	$+\frac{1}{2}$	-80	
	$1\nu^{-}2\pi^{-}$	-	$-\frac{1}{2}$	-23	-0.061
		-	$+\frac{1}{2}$	-13	
	$1\nu^{+}2\pi^{-}$	+	$-\frac{1}{2}$		> 0.600
		+	$+\frac{1}{2}$	15	

high frequency ω , but the negative-parity band does not.

B. The nuclei around ^{134}Ce

From the point of view of studying γ -polarization effects these nuclei have two advantages: the potential energy is presumably softer toward γ deformation than around ^{130}Ce , and also the additional neutrons lead to a situation of maximum conflict between neutron and proton $h_{11/2}$ rotation-aligned quasiparticles in the domain of collective rotation, $-60^{\circ} < \gamma < 0^{\circ}$. However, there are disadvantages from the proximity to the line of stability, which makes these lanthanums and ceriums inaccessible to heavier-ion reactions, and from the proximity to the $N=82$ closed shell, which makes it possible for noncollective modes to compete with collective rotation along the yrast line.^{32,35}

In the calculation for ^{134}Ce , the proton and neutron aligned bands come at about equal energy (Fig. 8). Experimentally, a g-factor measurement has established that it

is the neutron aligned band which is observed up to high spins.³² This is an unusual situation, since the $\nu h_{11/2}$ shell is half full. It suggests the possibility of observing the γ -inverse effect discussed in Sec. IIB above. The calculation for the one-quasiproton, two-quasineutron negative parity band does give almost zero signature splitting (Fig. 8). Thus ^{135}Pr , which is accessible to heavier-ion reactions than ^{133}La , emerges as a good case to look for the γ -inverse effect in experiment. There may be some difficulty in populating the interesting band since there are also several positive-parity bands along the yrast line. A study of ^{133}La by (α, xn) reactions does in fact indicate that the collective $(\pi h_{11/2})^1$ band is not yrast at $I = \frac{29}{2}$. However, in ^{134}Ce the collective band was populated to high spin by a $(^{16}\text{O}, 4n)$ reaction,³² although it is not yrast around $I = 10$.

For the odd-neutron case the calculation gives a reduction of the signature splitting almost to zero when the $h_{11/2}$ protons align (Fig. 8). This is the analog of the $^{81}\text{Kr}, ^{159}\text{Tm}$ effect, which might thus be observable in any

of the light odd-mass ceriums (cf. Fig. 5). The signature splitting is likewise calculated to be small in the yrast band of the doubly-odd cases, due to the same mechanism, in both Figs. 7 and 8.

V. SUMMARY AND CONCLUSIONS

The cranking term in the cranking Hamiltonian breaks the symmetry which otherwise would make it sufficient to consider one 60° sector of intrinsic quadrupole deformation space. Instead, one 60° sector is required for each of the three principal axes. Generally, such broken symmetries must be restored in a numerical simulation of laboratory-frame physics, but the physical picture is clearer in some respect prior to the restoration of symmetry. In Fig. 1, a simple physical picture is proposed for rotation-aligned high- j quasiparticles in the cranked intrinsic frame of reference. The spatial density distribution of the orbit varied smoothly and systematically through all three sectors, 180° in γ , if the filling of the shell is varied so that the character of the quasiparticle changes smoothly from that of a particle to a hole. This picture is founded on numerical results from cranking calculations described in Refs. 10 and 11.

When the nuclear γ deformation coincides with the particle γ deformation the favorable spatial overlap leads to a large signature splitting. Numerical results for the $h_{11/2}$ shell are displayed systematically in Ref. 11. Several authors are currently proposing that experimental signature splittings can be used to probe γ deformations,⁷⁻¹² and thus ultimately to justify the use of a cranked intrinsic representation. Some experimental findings have already been interpreted along these lines. The hypothesis still needs to be critically appraised both in experiment and within the collective model.

A priori one of the most promising regions for experimental tests is the light cerium region. An evaluation of the possibilities was carried out above, using a rudimentary model for γ deformations and signature splittings in the cranked intrinsic frame. The signature splitting of one-quasineutron $h_{11/2}$ bands is already known in the odd-mass light Ce isotopes, and a reduction of this split-

ting above the backband would be the analog of recent observations, e.g., in ^{81}Kr and ^{159}Tm . The same effect would lead to a reduced signature splitting in the yrast band of the doubly odd La or Pr isotopes. However, a previous analogous measurement in the Br isotopes, which are the doubly odd neighbors of ^{81}Kr , did not give this result.³⁶ The Br results have been taken to suggest that the signature splitting in doubly odd nuclei is determined primarily by residual interactions between the two quasiparticles rather than the Coriolis interaction due to the rotation of the mean field.³⁷

A new kind of situation might be studied in odd-mass La or Pr isotopes, because in these nuclei the alignment of quasiparticles which are halfway between particles and holes may be observable. The present calculation predicts a reduced signature splitting in the aligned band, the same as for the odd-mass ceriums, but due to a change of γ in the *opposite* direction. A favorable case to observe this " γ -inverse" effect is ^{135}Pr .

Some interesting points were noted in the course of determining empirical parameters for the present calculation. From the present model it emerges that the appropriate potential energy function for the lightest ceriums is intermediate between the stiffly prolate potential calculated with a single-particle potential of a folded-Yukawa type²⁷ and the very γ -soft potentials previously obtained from the modified oscillator and Woods-Saxon models.^{26,31} From experimental binding-energy data indications were found for an anomalous increase in the pairing gap for Z and N sufficiently far above 50 and below 82, respectively.

ACKNOWLEDGMENTS

Work at the University of Tennessee was supported by the U.S. Department of Energy under Contract No. DE-AS0576ER04936. UNISOR is a consortium of twelve institutions, supported by them and by the Office of Energy Research of the U.S. Department of Energy under Contract No. DE-AC05-76OR00033 with Oak Ridge Associated Universities.

*Permanent address: Institute of Atomic Energy, Academia Sinica, Peking, People's Republic of China.

†Permanent address: Central Institute for Nuclear Research, Rossendorf, German Democratic Republic.

¹P. Ring and P. Schuck, *The Nuclear Many-Body Problem* (Springer, New York, 1980).

²A. Bohr and B. R. Mottelson, *Nuclear Structure* (Benjamin, New York, 1975), Vol. 2.

³G. Andersson *et al.*, Nucl. Phys. **A268**, 205 (1976).

⁴K. Neergård, V. V. Pashkevich, and S. Frauendorf, Nucl. Phys. **A262**, 61 (1976).

⁵F. S. Stephens, Rev. Mod. Phys. **47**, 43 (1975).

⁶J. Meyer-ter-Vehn, Nucl. Phys. **A249**, 111 (1975); **A249**, 141 (1975).

⁷R. Bengtsson, F. R. May, and J. A. Pinston, in Proceedings of the XX International Winter Meeting on Nuclear Physics, Bormio, 1982, p. 144. Physics Dept., University of Milan,

1982.

⁸R. Bengtsson, J. A. Pinston, D. Barneoud, E. Monnard, and F. Schussler, Nucl. Phys. **A389**, 158 (1982).

⁹R. Bengtsson, in *High Angular Momentum Properties of Nuclei*, edited by N. R. Johnson (Harwood, New York, 1983), p. 161.

¹⁰S. Frauendorf and F. R. May, Phys. Lett. **125B**, 245 (1983).

¹¹G. A. Leander, S. Frauendorf, and F. R. May, in *High Angular Momentum Properties of Nuclei*, edited by N. R. Johnson (Harwood, New York, 1983), p. 281.

¹²B. R. Mottelson, in *High Angular Momentum Properties of Nuclei*, edited by N. R. Johnson (Harwood, New York, 1983), p. 1.

¹³S. Frauendorf and E. Sobeslavsky (unpublished).

¹⁴L. Funke *et al.*, Phys. Lett. **120B**, 301 (1983).

¹⁵J. D. Garrett *et al.*, Contribution to Nordic Meeting on Nuclear Physics, Fuglsø, 1982, p. 38. Niels Bohr Institute, 1982.

¹⁶L. L. Riedinger, Phys. Scr. (in press).

- ¹⁷H. Toki, H. L. Yadav, and A. Faessler, *Z. Phys. A* **292**, 79 (1979).
- ¹⁸J. Ludziewski *et al.*, *Nucl. Phys.* **A344**, 266 (1980).
- ¹⁹R. V. F. Janssens *et al.*, submitted to *Phys. Lett.*
- ²⁰I. Ragnarsson, in *Future Directions in Studies of Nuclei Far from Stability* (North-Holland, Amsterdam, 1980), p. 367.
- ²¹R. Bengtsson and S. Frauendorf, *Nucl. Phys.* **A327**, 139 (1979).
- ²²S. Frauendorf, *Proceedings of the ICPT Nuclear Physics Workshop, Trieste, 1981*, edited by C. H. Dasso (North-Holland, Amsterdam, 1981), p. 111.
- ²³S. G. Nilsson *et al.*, *Nucl. Phys.* **A131**, 1 (1969).
- ²⁴J. Gizon *et al.*, *Nucl. Phys.* **A290**, 272 (1977).
- ²⁵G. A. Leander, P. Arve, T. Bengtsson, I. Ragnarsson, and J. Y. Zhang, *Nucl. Phys.* **A400**, 97c (1983).
- ²⁶I. Ragnarsson *et al.*, *Nucl. Phys.* **A233**, 329 (1974).
- ²⁷P. Möller and J. R. Nix, *At. Data Nucl. Data Tables* **26**, 165 (1981).
- ²⁸A. Ansari, O. Civitarese, and A. Faessler, *Nucl. Phys.* **A334**, 93 (1980).
- ²⁹P. J. Nolan *et al.*, *Phys. Lett.* **108B**, 269 (1982).
- ³⁰S. Frauendorf, *Phys. Scr.* **24**, 349 (1981).
- ³¹U. Götz, H. C. Pauli, K. Alder, and K. Junker, *Nucl. Phys.* **A192**, 1 (1972).
- ³²M. B. Goldberg *et al.*, *Phys. Lett.* **97B**, 351 (1980), and references therein.
- ³³J. Dobaczewski and G. Leander, as quoted in Ref. 35.
- ³⁴P. J. Nolan *et al.*, in *High Angular Momentum Properties of Nuclei*, edited by N. R. Johnson (Harwood, New York, 1983), p. 57.
- ³⁵T. Morek *et al.*, *Nucl. Phys.* **A391**, 269 (1982).
- ³⁶L. Funke, *Proceedings of the International Symposium on Dynamics of Nuclear Collective Motion, Mount Fuji, 1982*, edited by K. Owaga and K. Tanabe (INS, University of Tokyo, 1982), p. 495.
- ³⁷G. Poggel, A. Faessler, and K. W. Schmid, *Z. Phys. A* **299**, 55 (1981).